ACS APPLIED MATERIALS & INTERFACES

Research Article

www.acsami.org

Nonfouling Tunable βCD Dextran Polymer Films for Protein Applications

Lars W. Städe,[†] Thorbjørn T. Nielsen,[†] Laurent Duroux,[†] Mogens Hinge,[‡] Kyoko Shimizu,[§] Leonid Gurevich,[⊥] Peter K. Kristensen,[⊥] Christer Wingren,[∥] and Kim L. Larsen*[,†]

[†]Department of Biotechnology, Chemistry and Environmental Engineering, Aalborg University, Frederik Bajers Vej 7H, DK-9220 Aalborg East, Denmark

[‡]Department of Engineering, Aarhus University, Finlandsgade 22, DK-8200 Aarhus, Denmark

[§]Department of Chemistry, Aarhus University, Langelandsgade 140, DK-8000 Aarhus, Denmark

[⊥]Department of Physics and Nanotechnology, Aalborg University, Skjernvej 4A, DK-9220 Aalborg East, Denmark

[∥]Department of Immunotechnology and CREATE Health, Lund University, Medicon Village, SE-22381 Lund, Sweden

Supporting Information

ABSTRACT: Polymeric β-cyclodextrin (βCD) films tunable with respect to thickness and βCD content were prepared in order to develop a suitable platform, allowing for inclusion of nonpolar guest molecules in the βCD cavity, while suppressing nonspecific protein adsorption. The βCD films were synthesized from linear βCD dextran polymers, and grafted onto silicon oxide surfaces by "click" chemistry. Topographic and morphological characteristics are controllable by reaction conditions and polymer type, with average film heights from 2.5 to 12.5 nm. Reversible introduction of electrostatic charges in the βCD dextran by complex formation with 1-adamantanecarboxylic acid prior to surface grafting resulted in a thinner and denser film, presumably by decompaction of the polymers. Total internal reflection fluorescence spectroscopy (TIRF) was employed to evaluate the accessibility of βCD cavities to the fluorescent probe 2-anilinonaphthalene-6-sulfonic acid. Only a minor fraction of the βCD cavities was accessible in the thicker and less dense films; however, accessibility was largely improved with increased ionic strength using NaCl up to 1 M. Antifouling properties of the βCD dextran polymer films were assessed by TIRF real-time monitoring, using bovine serum albumin as a model protein, and showed a 5- to 10-fold reduction in nonspecific adsorption as compared to a bare quartz surface with the degree of reduction reflecting film thickness and interfacial polymer density.

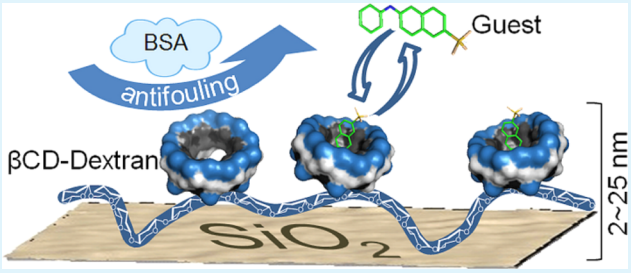

KEYWORDS: *β-cyclodextrin, dextran, polymer films, protein immobilization, nonspecific adsorption, total internal reflection fluorescence spectroscopy*

INTRODUCTION

The development of surfaces compatible with protein stability and function is a key issue in a wide range of biotechnological applications.[1,2] This concerns, for instance, applications as diverse as protein microarrays and medical implants. The general objective is to engineer desired surface characteristics while minimizing unwanted (nonspecific) interactions, as these may result in protein aggregation and denaturation.[1,3] For implants, these characteristics could involve the encapsulation of a relevant drug, e.g., an antibiotic for local delivery,[2] while for protein microarrays, the grafting of capture agents for site-selective immobilization is desired.[4] The unique feature of the cyclic oligosaccharide β-cyclodextrin (βCD) to host small lipophilic compounds in its cavity by host−guest inclusion complex formation has proved useful in this context. Facile modification, biocompatibility, low price, and high accessibility[5] make βCD an attractive surface host for protein immobilization[6−12] and drug delivery/release.[13−16] The latter of these two applications is by far the most extensively studied; however, there has been increased attention toward the use of βCD as capture agents for protein immobilization, e.g., for the development of protein microarrays.

Protein immobilization can be achieved by employing an orthogonal (bifunctional) linker, allowing for inclusion in the βCD cavity through host−guest interactions and binding to a protein or protein tag.[7,11,17−19] Alternatively, proteins chemically tagged with suitable βCD guest molecules can be immobilized directly onto βCD functionalized surfaces.[6,9,10,20] Our group has, in line with this approach, developed a method, termed, "Dock'n'flash" for light-induced covalent immobilization of proteins tagged genetically with a photoreactive βCD guest molecule.[8,21] The work presented here aims at designing βCD functionalized flat silicon oxide surfaces suitable for site-

Received: November 27, 2014
Accepted: January 31, 2015
Published: January 31, 2015

DOI: 10.1021/am508350r
ACS Appl. Mater. Interfaces 2015, 7, 4160−4168

specific immobilization of βCD guest-tagged proteins, and with minimal nonspecific protein adsorption.

The topic of protein immobilization and the requirements for suitable surfaces have been thoroughly and critically reviewed;[4,22] it was concluded that an ideal surface would consist of a thin organic film with a high density of available capture agents (in this context βCDs) for site-specific protein immobilization. Further, the coating should be "protein compatible" while suppressing nonspecific protein adsorption. "Protein compatibility" is a critical aspect in order to preserve structural and functional integrity of immobilized proteins (e.g., avoid denaturation).[4,22] Antifouling is equally critical to prevent interference and passivation from nonspecifically adsorbed proteins during immobilization and applications of the surfaces.[4,22,23] Finally, the method should lead to high reproducibility, high coupling yields, and a stable surface chemistry in order to ensure maximum and uniform surface coverage as well as to alleviate losses of immobilized protein during washing steps.[4,22]

Silicon oxide surfaces are attractive for protein immobilization, as glass and quartz permit the use of optical techniques, while oxidized silicon wafers (Si) are well suited for a range of surface characterization techniques, including ellipsometry and scanning probe microscopy (SPM).[4,22,23] Grafting of βCD onto these materials has been addressed in numerous studies, typically by coupling of mono- or poly-substituted βCD to a reactive moiety of an alkane silane after silanization of the surface.[10,11,20,24−26] Although several of the reported methods have been applied successfully for protein immobilization,[10,11,20] the performance of the functionalized surfaces with respect to nonspecific protein adsorption of abundant serum proteins has received less attention. This issue was nevertheless addressed in a study on immobilization of proteins onto self-assembled monolayers of per-substituted βCD heptathioether on gold surfaces.[17] In this study, significant nonspecific adsorption of streptavidin, bovine serum albumin (BSA), and histidine-tagged maltose binding protein onto the βCD functionalized surfaces was reported.[17] Although the study concerns planar gold surfaces it highlights the necessity of rendering the βCD modified surface resistant to nonspecific protein adsorption prior to protein immobilization. This was efficiently achieved by the authors of the relevant study by pretreating the βCD modified surfaces with adamantane modified oligo(ethylene glycol),[17] which could be coadded or replaced with bifunctional adamantane linkers, thereby facilitating subsequent protein immobilization.[17]

Alternatively, nonspecific protein adsorption may be addressed by having the βCD incorporated into an antifouling polymer, thereby avoiding additional pretreatments prior to protein immobilization. The natural polysaccharide dextran is in this respect a promising scaffold for anchoring of βCD, as previous studies have shown that dextran polymer coated surfaces efficiently suppress nonspecific protein adsorption and prevent protein aggregation.[27−29] βCD dextran (Dβ CD) polymers may consequently provide a protein compatible coating, shielding the underlying substrate and the chemistry facilitating surface functionalization, while simultaneously allowing for βCD host−guest interactions.

In the present study, we made use of a recently developed approach for the synthesis of linear Dβ CD polymers prepared from native dextran by "click" chemistry.[30] Here, Dβ CD polymers were prepared from 5 and 110 kDa dextran (D5βCD and D110βCD) and grafted onto azido functionalized quartz and Si slides by a copper(I)-catalyzed azide−alkyne cycloaddition (CuAAC). Changes in film structuration in response to surface grafting of the polymers at varying concentration and in the presence/absence of a high affinity βCD guest molecule were investigated using SPM and ellipsometry. By employing the sensitive surface technique total internal reflection fluorescence (TIRF) spectroscopy, the observed changes in structuration were related to the accessibility of βCD for inclusion complex formation and to the antifouling properties of the polymer films.

EXPERIMENTAL SECTION

Materials. Polished CZ Si wafers (P/boron doped; diameter, 200 mm; orientation, {100}; sheet resistance, 5−20 Ω/sq; thickness, 710−740 μm) were obtained from SEH Europe Ltd. (West Lothian, UK) and diced in 10 × 10 mm slides. Quartz slides (25 × 38 × 1 mm) were purchased from TIRF Labs Inc. (Morrisville, NC, USA). PEG400 and DMSO (VWR International, Fontenay-sous-Bois, France), 2-anilinonaphthalene-6-sulfonic acid (2,6 ANS, Invitrogen, Oregon, USA) were all used as received. 6-Monodeoxy-6-monoazido-βCD (N_3βCD, Nielsen et al.[30]), propargyl modified 5 and 110 kDa dextran (D5GP and D110GP, Nielsen et al.[30]), and (tris(benzyltriazolylmethyl)amine (TBTA, Chan et al.[31]) were prepared according to the literature. All other chemicals were obtained from Aldrich (Steinheim, Germany).

General Procedures (for Details, See the Supporting Information). NMR analyses were conducted in D_2O with a Bruker DRX600 spectrometer equipped with a 5 mm TXI (H/C/N) xyz-gradient probe. Ellipsometric measurements were conducted with a Sentech SE 850 ellipsometer. Polarization modulation infrared reflection absorption spectroscopy (PM-IRRAS) spectra were collected on a Nicolet 6700 FT-IR equipped with a photoelastic modulator (PEM 90). X-ray photoelectron spectroscopy (XPS) analysis was achieved using a Kratos Axis Ultra-DLD spectrometer. Surface topography and morphology were visualized by SPM on a NTEGRA Aura operated in intermittent contact mode. TIRF spectroscopy was performed on a Varian Cary Eclipse fluorescence spectrophotometer equipped with a TIRF Labs flow system.

Synthesis of βCD Polymers. 0.25 g of the D5GP and D110GP (0.22 and 0.27 mmol alkynes, respectively), N_3βCD (0.8 equiv), sodium ascorbate (0.15 equiv), and TBTA (0.055 equiv) were dissolved in 25 mL of oxygen free DMSO/H_2O (1:1) under a nitrogen atmosphere. $CuSO_4$ (0.05 equiv) was added, and the solution was stirred for 2 h at 50 °C and subsequently precipitated in 300 mL of acetone. The crude polymers were dissolved in 50 mL of water and swirled over 2 g of Ambersep GT74 resin for 12 h and dialyzed for 72 h (MWCO 3.5 kDa, Spectrum Laboratories Inc., CA, USA). The pure polymers were obtained as white solids by lyophilization (yield 69−82%).

Surface Activation. Cleaned and hydroxylated quartz and Si slides were silanized with 3-glycidoxypropyltrimethoxysilane (GPTMS) by vapor deposition at −800 mbar for 48 h at 105 °C after which, azide functionalities for the CuAAC were introduced by ring opening of the epoxides with 400 mM sodium azide in PEG400[32] for 4 h at 40 °C (for details, see the Supporting Information). Following azidolysis, the substrates were rinsed thoroughly with Milli-Q water (MQ), sonicated for 5 min in EtOH, and dried under a stream of dry nitrogen. Quartz substrates were immediately transferred to a nitrogen purged glovebox, while Si slides were kept under argon until measured by ellipsometry and then transferred to the glovebox.

Surface Grafting. All surface CuAAC reactions were conducted in the glovebox at 40 °C with reagents degassed and nitrogen purged (for details, see the Supporting Information). Briefly, quartz and Si substrates to be processed alike were placed in the same reaction dish on an orbital shaker facing front up and the appropriate polymer solution added. The volume was adjusted to 6 mL with DMSO/MQ (1:1) and then TBTA (60 μM), $CuSO_4$ (50 μM), and sodium ascorbate (150 μM) were added in the listed order. After 2 h, the slides were rinsed with DMSO/MQ (1:1) and the CuAAC reaction

DOI: 10.1021/am508350r
ACS Appl. Mater. Interfaces 2015, 7, 4160−4168

Scheme 1. (a) Synthesis of Linear DβCD Polymers from Propargyl Modified Dextrans onto which $N_3\beta$CD is Grafted by "Click" Chemistry. (b) Grafting of the DβCD Polymers onto Azido Functionalized Silicon Oxide Surfaces by "Click" Chemistry

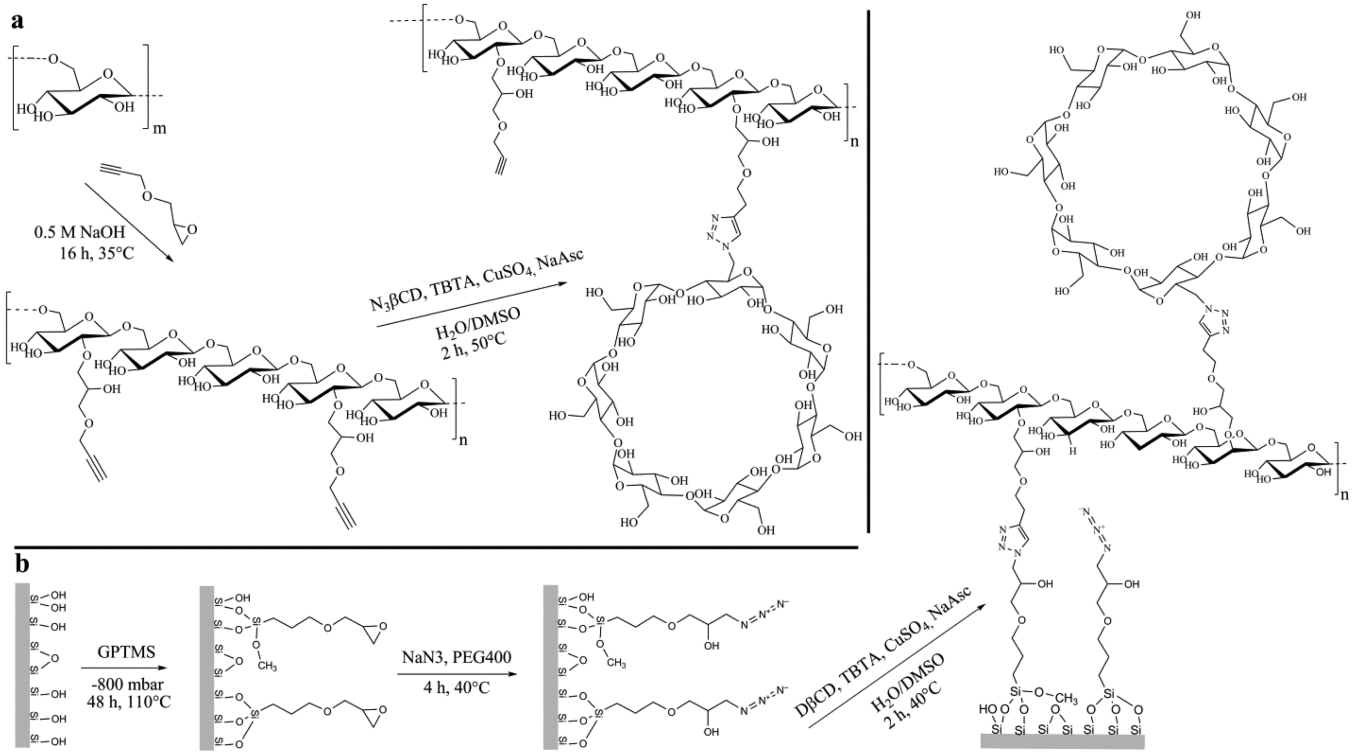

repeated twice, first with $N_3\beta$CD (step excluded for D110GP polymer) and then with propargyl alcohol instead of the polymers. The slides were then transferred from the glovebox and sonicated 20 min in DMSO, DMSO/MQ (1:1), and MQ. Quartz slides were subsequently stored in MQ, while Si slides were dried under a mild stream of dry nitrogen.

Inclusion Complex Formation. To probe βCD accessibility, the appropriate quartz slide was mounted and fluorescence emission spectra (340 to 625 nm at λ_{ex} 320 nm) recorded after injection of 250 μL of 1 mM 2,6-ANS in PBS (10 mM, pH 7.4) with or without 1 M NaCl.

Protein Adsorption. The BSA adsorption measurements were conducted by mounting the appropriate quartz slide, injecting PBS and heating the slide to 37 °C at which point continuous emission recording (λ_{ex} 555 nm, λ_{em} 565 nm) was initiated. After 60 to 120 s, the PBS was replaced with 250 μL of 0.4 mg/mL Alexa Fluor 555 labeled BSA (DOL 0.6) in PBS (50 μL/s), freshly prepared from an ice cold stock solution in PBS. The same stock solution was used for all slides and all measurements were conducted within 4 days. After 60 min of incubation with the labeled BSA, the flow cell was flushed with 5 × 2.5 mL PBS (166 μL/s).

RESULTS AND DISCUSSION

Synthesis and Grafting of DβCD Polymers. The synthesis of the DβCD polymers is illustrated in Scheme 1a. The synthesis is based on the method described by Nielsen et al.[30] Propargyl modified dextrans, D5GP and D110GP, were grafted with $N_3\beta$CD by CuAAC to give D5βCD and D110βCD however, using only 0.8 equiv of $N_3\beta$CD per alkyne, in order to retain free alkynes for subsequent CuAAC surface grafting. Table 1 provides the average number of free alkynes and βCD units of the surface grafted polymers calculated from the average molecular weight of the dextran and the molar ratios of βCD and alkynes. The ratio of free alkynes was determined by ^{1}H NMR (NMR spectra in the Supporting Information, Figures S1 to S3).

Table 1. Specifications of Polymers Used for Grafting

polymer	Ave MW (kDa)	glucose units[a]	alkyne ratio[b]	βCD ratio	ave. # alkynes	ave. # βCD
D110GP	127	679	0.22	N/A	149	N/A
D5βCD	133	31	0.27	0.8	1.6	7
D110βCD	260	679	0.22	0.8	30	120

[a]Based on the molecular weight of the dextran polymers. [b]Molar ratio of free alkynes as determined by ^{1}H NMR.

The introduction of azides for CuAAC grafting of the polymers (Scheme 1b) was done in two steps. First, the cleaned substrates were silanized with GPTMS by vapor deposition; second, azidolysis of the epoxides was achieved with sodium azide in PEG400. The average thickness of the azidosilane layers determined from ellipsometry, assuming bulk refractive indices of the natural grown oxide and the silane monolayer, yields 0.8 ± 0.1 nm. Compared to a fully extended length of 0.95 nm for GPTMS,[33] the obtained thickness of the silane layers indicates the formation of incomplete monolayers. This is attributed to the reaction conditions which, in the absence of H_2O, disfavor hydrolysis and polymerization of the silanes. Therefore, silanes only react with surface silanols resulting in noncontinuous films. The final steps in surface functionalization are the CuAAC surface grafting of the polymers (Scheme 1b) followed by saturation of unreacted surface azides and alkynes on the dextran backbone with propargyl alcohol and $N_3\beta$CD, respectively (not shown in Scheme 1b). The CuAAC used for both synthesis and surface grafting is known to be selective, proceed fast and react quantitatively under mild conditions and the formed triazole is stable against oxidation, reduction, and hydrolysis.[34] The CuAAC is therefore considered suitable both

DOI: 10.1021/am508350r
ACS Appl. Mater. Interfaces 2015, 7, 4160−4168

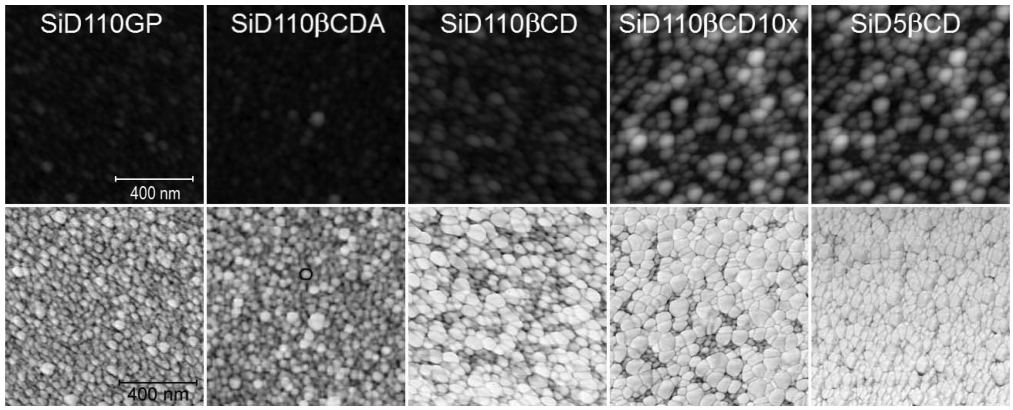

Figure 1. SPM (1 × 1 μm) topographical (top) and phase imaging (bottom) of the five types of polymer films. The vertical scale for the topographical images is 0−30 nm.

for controlling βCD ratio of the DβCD polymers and to achieve full coverage with a stable surface coating.

The presence of characteristic βCD IR absorption frequencies and the expected change in chemical composition upon surface grafting of the DβCD polymers were confirmed by PM-IRRAS and XPS, respectively (spectra and assignment in the Supporting Information). With the three polymers (Table 1), five types of films were prepared. To investigate the effect of the incorporation of βCD on the resulting film properties, the D110GP and the D110βCD polymers were grafted at the same molar concentration (2 μM), and the D110βCD polymer was additionally grafted in complex with the high-affinity βCD guest molecule, 1-adamantanecarboxlic acid (Ada-COO$^-$, log K 4−4.5).[35] Further, the concentration dependency was probed by grafting the D110βCD polymer at a 10-fold higher polymer reaction concentration (20 μM). Finally, films were prepared with the short chain D5βCD polymer to investigate the effect of single-point vs multipoint attachment, as this polymer has only 1.6 alkynes on average available for surface grafting compared to an average of 30 for the D110βCD polymer (Table 1). The polymer films will, for further reference, be labeled according to type of slide (Q, Si), polymer used, and, for the D110βCD polymer films, an indication of the presence of Ada-COO$^-$ (A) during surface grafting or the 10-fold polymer reaction concentration (10×). For example, film SiD110βCDA is prepared from the polymer D110βCD grafted onto a Si slide in the presence of Ada-COO$^-$.

Surface Characterization. The polymer films were characterized by SPM and ellipsometry to gain insight into the change in surface structuration in response to the different reaction conditions. From the SPM imaging, and in particular the phase imaging (Figure 1, bottom panel), it is evident that for all of the prepared films, the grafting results in excellent coverage of the Si substrates with densely packed polymer assemblies. There are, however, noticeable differences in topographical and morphological appearances. Films SiD110GP and SiD110βCDA are constituted of structures best described as hemispherical and have almost identical, narrow unimodal height distributions (Figure 2) and roughness values below 1 nm. The structure marked with a circle on the phase imaging for SiD110βCDA (Figure 1, second panel from bottom left) represents the typical structure observed on both SiD110GP and SiD110βCDA. Its projected boundary length and calculated volume (based on a Laplacian background) are

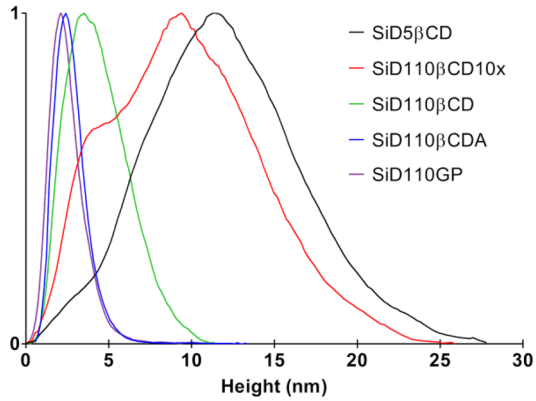

Figure 2. Normalized height distribution plots extracted from the topographic (1 × 1 μm) SPM measurements (Figure 1).

129 and 490 nm^3, respectively. Assuming an average distance of 0.7 nm between each D-glucose unit[36] constituting the dextran backbone of the D110 polymer, its calculated length in fully extended conformation is ∼475 nm. With this crude estimate in mind, the apparent volume of 490 nm^3 may correspond to one single polymer chain. The hemispherical structuration is ascribed to strong intramolecular H-bonding between the dextran −OH groups, in accordance with a previous study on D10 dextran films showing that similar hemispherical assemblies decompose and spread onto the surface in response to increased oxidation of the dextran chain.[29] It was suggested that the hemispherical structuration could be the result of either the collapse of dextran chains due to strong collective intramolecular H-bonding interactions between the −OH groups, or the result of the polymers adapting a "tail" conformation due to the fact that the "native" dextrans had only one site for surface grafting.[29] The polymers used for SiD110GP and SiD110βCDA have in average 147 and 20 free alkynes available for surface grafting (Table 1). The similarity of these two films, in spite of the large difference in total number of alkynes indicates that it is, in fact, intramolecular interactions and not the number of free alkynes, i.e., potential grafting sites, which are the dominant factors responsible for the hemispherical structuration.

The appearances of films SiD110βCD, SiD110βCD10x, and SiD5βCD are distinctively different from films SiD110GP and SiD110βCDA by being dominated by large bead-shaped polymer assemblies, varying in shape, packing density, height,

DOI: 10.1021/am508350r
ACS Appl. Mater. Interfaces 2015, 7, 4160−4168

and height distribution. The origin of these large polymer assemblies is revealed by comparing film SiD110βCD and SiD110βCDA, for which the only difference in preparation is the addition of the high-affinity βCD guest molecule Ada-COO$^-$ to the polymer solution prior to surface grafting of the latter of the films (Ada-COO$^-$ displaced after grafting by post-treatment). The almost complete absence of large polymer assemblies on film SiD110βCDA shows that the presence of Ada-COO$^-$ (in complex with βCD) disturbs the formation of these assemblies and thereby favors coupling of individual polymer strands, presumably through more grafting points. This effect is ascribed to the inclusion of Ada-COO$^-$ into the βCD cavity disturbing βCD driven intermolecular interactions through electrostatic repulsion by the carboxylate groups, resulting in decompaction.

The presumed increased density of polymer chains at the interface, due to better spreading, suggested for film SiD110βCDA is supported by the comparison between SPM and the ellipsometric measurements (Table 2). The ellipsometric thickness estimation of film SiD110GP correlates with the average height extracted from the SPM imaging, indicating that the assigned refractive index of 1.5, obtained from the literature,[37] is appropriate for this film. The slightly overestimated ellipsometric thickness obtained for film SiD110βCDA may reflect an increase in the refractive index in response to the βCD grafting or the presence of nondisplaced Ada-COO$^-$, and/or be ascribed to the presence of a minor population of large polymer assemblies, similar to those observed on film SiD110βCD/10x (due to grafting of non- or partial complexed D110βCD polymers). More interestingly, however, is the notable underestimated ellipsometric thicknesses obtained on films SiD110βCD, SiD110βCD10x, and SiD5βCD, for which the deviation increases (Table 2) as the larger bead-shaped polymer assemblies become dominant on film appearance (Figure 1) and the average film heights and height distributions increase (Figure 2). This is indicative of a decrease in the effective refractive index of these three films compared to film SiD110βCDA, because the bulk refractive index of the polymers must be comparable (unambiguously for the D110βCD films). Alternatively, it is the result of blank spots, i.e., areas free of polymers on these films. This is, however, contradictive in light of the higher polymer reaction concentrations used for SiD110βCD10x and SiD5βCD and the fact that a 20 × 20 μm SPM scan on film SiD110βCD10x confirms full surface coverage (Supporting Information, Figure S6). Consequently, it is concluded that the large polymer assemblies are constituted of loosely packed DβCD polymer strands formed by the aforementioned βCD driven intermolecular interactions. The reduced compactness of these assemblies effectively lowers the refractive index of the films as compared to films SiD110βCDA and SiD110GP. Further, that film SiD110βCD yields a slightly lower ellipsometric thickness than SiD110βCDA indicates that the latter film has, in fact, a higher density of DβCD in spite of SPM imaging showing a notable thinner film thickness (Figure 1 and Table 2).

Table 2. Film Thicknesses (ΔT) and Average Heights (h) Determined by Ellipsometry and SPM, Respectively

film	ΔT^a (nm)	h^b (nm)
SiD110GP	2.1 ± 0.2	2.5
SiD110βCDA	3.4 ± 0.2	2.8
SiD110βCD	3.1 ± 0.2	4.5
SiD110βCD10x	5.6 ± 0.4	9.9
SiD5βCD	7.3 ± 0.3	12.2

[a]Average of six measurements. [b]Average film heights extracted from the SPM imaging (Figure 1).

These findings allow for an evaluation of the concentration dependent surface structuration observed for the D110βCD polymer on films SiD110βCD and SiD110βCD10x. Although the only difference in preparation of these films is the 10-fold higher polymer concentration, i.e., 2 vs 20 μM (0.5 vs 5 mg/mL), there are notable differences in film thicknesses (Table 2) and height distributions (Figure 3). At high polymer concentrations (SiD110βCD10x), competition for surface azides is likely to be promoted. Consequently, the polymers are grafted through a lower number of attachment points, thereby adopting a conformation stretched in the z-dimension, i.e., higher film height, giving rise to a high proportion of the bead-shaped polymer assemblies (constituted of loosely packed polymer strands) with a wide height distribution. In comparison, at lower polymer concentration (SiD110βCD) reduced competition for surface azides is expected, thereby allowing more grafting points. This results in a thinner and denser film, i.e., smaller ellipsometric deviation with a sharper and almost unimodal height distribution.

The last film, SiD5βCD, differs by being prepared from a significant shorter dextran chain (~22 nm in fully extended

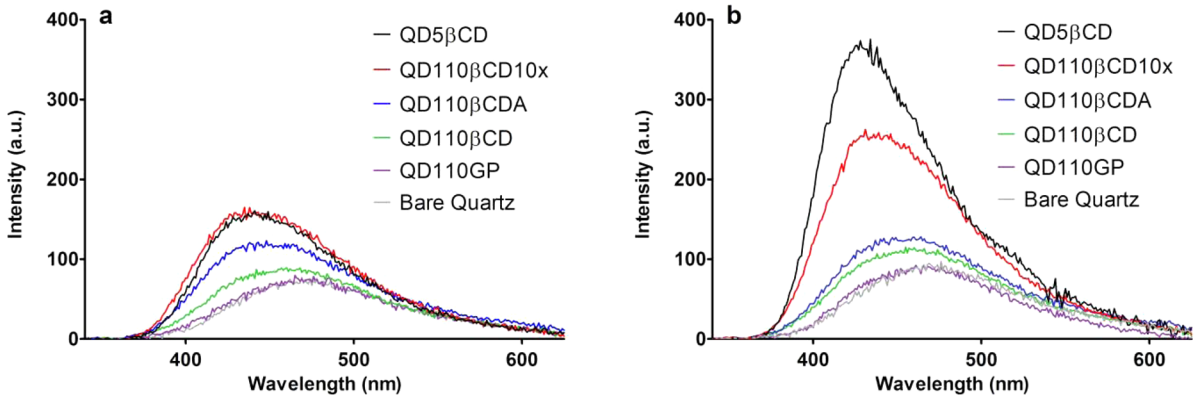

Figure 3. TIRF emission scans of the polymer films and a bare quartz slide after injection of 1 mM 2,6 ANS in PBS (pH 7.4) without (a) and with 1 M NaCl. (b). Excitation at 320 nm and buffer background subtracted.

DOI: 10.1021/am508350r
ACS Appl. Mater. Interfaces 2015, 7, 4160−4168

conformation). This film is characterized by displaying the thickest film (Table 2) and broadest height distribution (Figure 2). These features are thought to be the result of the D5βCD polymer having only 1−2 alkyne groups in average available for surface grafting (vs ∼30 for D110βCD). As a result of the limited grafting points, the polymer assemblies appear as extended in the *z*-direction with the height depending on the position of the alkyne(s) in the polymer chain. The alkyne substitution is expected to be randomly distributed, leading to a broad height distribution. Further, it should be noted that structuration/appearance of the D5βCD polymer is independent of polymer reaction concentration (0.5 to 5 mg/mL) and not affected by the presence of Ada-COO^- during grafting (not shown).

Taken together, these results show that DβCD polymers can be efficiently coupled to silicon oxide surfaces to yield nanometer-thick films of densely packed polymer beads, and ensuring excellent coverage of the substrate surface. The method thereby addresses the issue of low coupling yields often associated with "grafting to" techniques.[29,38] Obviously, film thickness can be tuned with the choice of reaction concentration (D110βCD) and backbone polymer (D110βCD vs D5βCD). More interestingly, the introduction of repulsive negative charges through host−guest complex formation between Ada-COO^- and the βCD cavities, leads to an improved spreading of the D110βCD polymer across the surface. Better shielding of the underlying substrate and surface chemistry is highly relevant with respect to suppression of protein adsorption.[28]

Inclusion Complex Formation. The relative accessibility of βCD cavities available for inclusion complex formation was evaluated for the five types of films using TIRF spectroscopy and the fluorescent probe 2,6-ANS as guest molecule. TIRF spectroscopy is a sensitive surface technique allowing for monitoring fluorescent events within ∼200 nm of the interfacial region and which physical design excludes potential interference from light-scattering events of the source beam (illustration of principal setup in the Supporting Information, Figure S7). With its coplanar aromatic rings, 2,6-ANS makes an excellent guest molecule for the βCD cavity (∼log *K* 3.3).[39] In water, 2,6-ANS displays only weak fluorescence due to the dipolar nature of water acting as an effective quencher but upon inclusion in the hydrophobic βCD cavity the fluorescence yield increases accompanied by a blue shift of the emission maximum.

Figure 3 shows the emission spectrum after injection of 1 mM 2,6-ANS in PBS buffer without (a) and with (b) an additional 1 M NaCl added for the five different types of films and a clean unmodified quartz surface. No change in fluorescence emission is observed for film QD110GP compared with the bare slide indicating that the propargyl modified dextran polymer backbone has no impact on 2,6-ANS fluorescence. On the contrary, the films prepared with DβCD polymers all display an increase in fluorescence intensity (FI) accompanied by a blue-shift in emission maximum thereby verifying the inclusion of 2,6-ANS in βCD cavities.

The most striking observation, however, is the strong enhancement in FI (and blue shift) in response to the presence of 1 M NaCl in the 2,6-ANS solution (Figure 3b) observed for film QD5βCD (black) and QD110βCD10x (red) and, to a lesser extent, film QD110βCD (green). These films correspond to the films for which SPM showed large bead-shaped polymer assemblies. This enhancement of the FI was found to be concentration dependent with an increase in FI up to 1 M NaCl, above which no further effect was observed (not shown). This effect is not observed on film QD110βCDA (blue) nor for the inclusion complex formation of free βCD and 2,6-ANS (Supporting Information, Figure S8). This indicates that the FI enhancement does not reflect a change in binding affinity, but instead can be ascribed to an increased number of binding events due to increased accessibility of βCD cavities to 2,6-ANS. This apparent limited accessibility of βCD cavities to 2,6-ANS in film QD5βCD, QD110βCD10x, and QD110βCD is surprising given that 2,6-ANS is a small diffusible molecule and the TIRF sensorgrams reached a steady signal seconds after injection of the fluorescent probe. Either the packing of the polymer assemblies would appear to be tight enough to form a molecular sieve preventing 2,6-ANS to reach buried βCD cavities or alternatively the secondary rims of βCD cavities are involved in H-bonding networks with each other, or the dextran backbone, preventing the binding of 2,6-ANS. Of these two explanations, the latter seems the more likely, as tight packing of the polymer assemblies is contradicted by the ellipsometric measurements, which indicated a loose structuration of the three films for which the presence of NaCl increases accessibility. In particular, βCD rim-rim interactions would explain the efficient shielding of the βCD cavities. In this context, it should be noted that free βCD tends to self-organize and to form βCD rim−rim interactions and that previous studies have shown that these interactions are suppressed by NaCl.[40−42] Ionic species have a direct effect on the structure on H-bonding network in water measured by their Jones−Dole B-coefficient.[43] Na^+ with a negative Jones−Dole B-coefficient acts as an H-bond breaker, whereas Cl^- with a positive Jones−Dole B-coefficient acts as an H-bond maker. With the magnitude of this coefficient being much higher for Na^+ than for Cl^-,[43] the H-bond breaking properties of Na^+ will predominate. It is anticipated that a high concentration of Na^+ in the solvent disrupts βCD H-bonding through similar mechanisms, resulting in decompaction and leading to higher accessibility to βCD cavities in film SiD110βCD, SiD110βCD10x, and SiD5βCD (Figure 3). The effect is thereby similar to that achieved when the D110βCD polymer is grafted in a complex with Ada-COO^- (Si/QD110βCDA) where charge repulsions are postulated to have resulted in H-bonding disruption, leading to decompaction and improved spreading of the film across the surface as observed on film SiD110βCDA (Figure 1). Consequently, βCD accessibility on the corresponding film QD110βCDA is not affected by treatment with 1 M NaCl (Figure 3), as this film is already in decompacted conformation and the βCD cavities are already solvent accessible after surface grafting.

Concerning the relative number of βCD cavities accessible for inclusion complex formation, the TIRF measurements correlate well with the findings in the surface characterization: the most intense FI enhancement is observed for QD5βCD and QD110βCD10x, in line with the thick films observed by SPM on the corresponding Si surfaces (Figure 1). For film QD110βCDA, TIRF spectroscopy reveals a higher density of accessible βCD cavities than film QD110βCD despite SPM indicating a thicker film for the corresponding SiD110βCD. This is, however, in line with the film densities estimated by ellipsometry. Finally, it should be noted that extended storage of the polymer grafted quartz slides in MQ water and repeated washing with PBS and EtOH did not change 2,6-ANS fluorescence response in subsequent injections (not shown), thereby confirming the stability of the grafted polymer films.

DOI: 10.1021/am508350r
ACS Appl. Mater. Interfaces 2015, 7, 4160−4168

Protein Adsorption. The films were probed with respect to nonspecific protein adsorption by monitoring real-time adsorption of fluorophore-labeled BSA with TIRF spectroscopy. BSA is structurally very similar to its human homologue, which is the most abundant protein in blood plasma, and contains multiple hydrophobic binding sites for nonspecific binding of hydrophobic molecules such as lipids.[44] Therefore, BSA is a relevant model for applications involving the exposure to blood plasma/serum. The experiments were conducted by injecting the fluorophore-labeled BSA (0.4 mg/mL), incubating for 60 min at 37 °C, and flushing repeatedly with PBS buffer, whereby the residual FI signal reflect different amounts of BSA adsorbed on the films.

The adsorption results of all films investigated are summarized in Figure 4 and gives the residual FI expressed as a percentage of the average FI for the last 2 min before the PBS flushing is initiated. Compared to the blank slide, which retains 9.4% of the initial FI signal, all of the polymer grafted slides suppress adsorption of BSA. However, there are notable differences in residual FI with the following ranking: QD110GP (0.03%) < QD110βCDA (0.7%) < QD110βCD (1.5%) < QD110βCD10x (2%) < QD5βCD (2.5%). This ranking mirrors the suggested grafting behavior, i.e., the more the grafting sites, the higher the interfacial polymer density, and the better the suppression of protein adsorption, in agreement with previous findings on dextran coated surfaces.[27,28] This is best exemplified with film QD110GP, which suppresses BSA adsorption more efficiently than film QD110βCDA, although the corresponding films on Si slides appear almost identical with respect to topographical and morphological appearance; in the absence of βCD, the D110GP polymer has 80% more alkynes and is likely to be coupled through significantly more grafting points. That it is the interfacial polymer density, i.e., number of grafting points, and not the presence of βCD that is the major determinant on nonspecific adsorption of BSA is evident from the fact that film QD110βCD displays higher protein adsorption than QD110βCDA (Figure 4), although QD110βCD has less βCD cavities accessible for inclusion complex formation (Figure 3) and thereby less solvent exposed βCD to interact with the BSA.

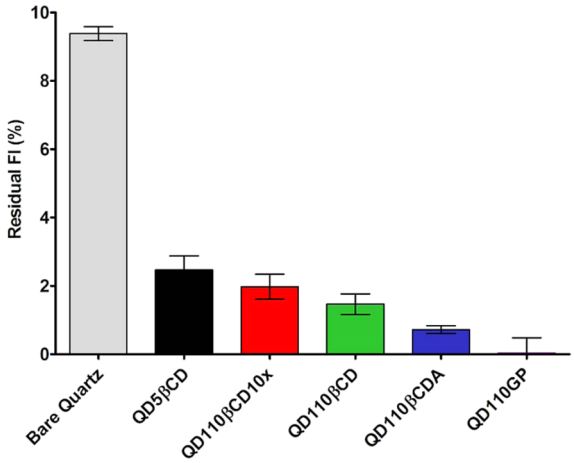

Figure 4. Nonspecific adsorption of Alexa Flour 555 labeled BSA onto the prepared films and a clean unmodified (hydroxylated) quartz slide measured by TIRF real-time monitoring. The residual FI is expressed as a percentage of the average FI for the last 2 min before PBS flushing is initiated.

CONCLUSION

In this study, the development of βCD functionalized silicon oxide surfaces allowing for host−guest interactions with nonpolar guest molecules, while suppressing nonspecific protein adsorption, was addressed. The proposed solution is based on synthesis of dense polymeric βCD monolayer films using dextran as a polymeric backbone. The DβCD polymers are prepared and grafted by "click" chemistry, allowing for mild reaction conditions, stable surface chemistry, and excellent surface coverage, and thereby shielding of the substrate and the alkane linker moieties, even when grafting at low polymer concentrations. The surface structuration of the polymers, and thereby film thickness and density, is tunable presumably by regulation of the number of surface grafting points and intermolecular H-bonding. Using TIRF spectroscopy, it is shown that the βCD cavities are available for host−guest interaction and that the polymer films suppress nonspecific protein adsorption with efficiencies depending on film structuration. Based on these results and previous findings, showing that dextran polymer coatings prevent protein aggregation, these films are considered "protein-friendly" and, consequently, suitable for protein applications. Concerning the intended application, namely platforms for protein immobilization based on βCD host−guest interactions, film Si/QD110βCDA is considered the most promising candidate due to the full accessibility to the βCD cavities, the low BSA adsorption, and the thin and smooth film appearance. Immobilization studies using the "Dock'n'flash" technology and single chain variable fragments antibodies tagged genetically with a photoreactive βCD guest-tag[21] are currently in progress. Although the thick DβCD films might be less suitable for protein immobilization, these may be relevant as surface coatings onto materials for medical implants, e.g., hydroxyapatites, for high-capacity delivery/release of drugs fitting the βCD cavity.

ASSOCIATED CONTENT

Supporting Information

(1) Detailed experimental procedures for instrumentation, surface activation, and grafting; (2) ^{1}H NMR spectra of the D110GP, D110βCD and D5βCD polymers used for grafting; (3) PM-IRRAS and XPS spectra of film SiD110βCD10x and detailed assignment; (4) SPM (20 × 20 μm) imaging of film SiD110βCD10x; (5) illustration of principal setup for TIRF spectroscopy; (6) NaCl effect on inclusion complex of 2,6-ANS and free βCD. This material is available free of charge via the Internet at http://pubs.acs.org.

AUTHOR INFORMATION

Corresponding Author

*K. L. Larsen. E-mail: kll@bio.aau.dk.

Notes

The authors declare no competing financial interest.

ACKNOWLEDGMENTS

FeF Chemicals, Køge, Denmark, the Swedish Research Council (VR-NT, grant to C.W.) and the Obel Family Foundation, Denmark (TIRF instrumentation, grant to L.D.) are kindly acknowledged for their financial support.

DOI: 10.1021/am508350r
ACS Appl. Mater. Interfaces 2015, 7, 4160−4168

REFERENCES

(1) Kasemo, B. Biological Surface Science. *Surf. Sci.* **2002**, *500*, 656−677.

(2) Hildebrand, H.; Blanchemain, N.; Mayer, G.; Chai, F.; Lefebvre, M.; Boschin, F. Surface Coatings for Biological Activation and Functionalization of Medical Devices. *Surf. Coat. Technol.* **2006**, *200*, 6318−6324.

(3) Senaratne, W.; Andruzzi, L.; Ober, C. K. Self-Assembled Monolayers and Polymer Brushes in Biotechnology: Current Applications and Future Perspectives. *Biomacromolecules* **2005**, *6*, 2427−2448.

(4) Rusmini, F.; Zhong, Z.; Feijen, J. Protein Immobilization Strategies for Protein Biochips. *Biomacromolecules* **2007**, *8*, 1775−1789.

(5) Singh, M.; Sharma, R.; Banerjee, U. Biotechnological Applications of Cyclodextrins. *Biotechnol. Adv.* **2002**, *20*, 341−359.

(6) Fragoso, A.; Caballero, J.; Almirall, E.; Villalonga, R.; Cao, R. Immobilization of Adamantane-Modified Cytochrome C at Electrode Surfaces through Supramolecular Interactions. *Langmuir* **2002**, *18*, 5051−5054.

(7) Ludden, M. J.; Péter, M.; Reinhoudt, D. N.; Huskens, J. Attachment of Streptavidin to β-Cyclodextrin Molecular Printboards via Orthogonal Host−Guest and Protein−Ligand Interactions. *Small* **2006**, *2*, 1192−1202.

(8) Jensen, R. L.; Städe, L. W.; Wimmer, R.; Stensballe, A.; Duroux, M.; Larsen, K. L.; Wingren, C.; Duroux, L. Direct Site-Directed Photocoupling of Proteins onto Surfaces Coated with β-Cyclodextrins. *Langmuir* **2010**, *26*, 11597−11604.

(9) Yang, L.; Gomez-Casado, A.; Young, J. F.; Nguyen, H. D.; Cabanas-Danés, J.; Huskens, J.; Brunsveld, L.; Jonkheijm, P. Reversible and Oriented Immobilization of Ferrocene-Modified Proteins. *J. Am. Chem. Soc.* **2012**, *134*, 19199−19206.

(10) Uhlenheuer, D. A.; Wasserberg, D.; Haase, C.; Nguyen, H. D.; Schenkel, J. H.; Huskens, J.; Ravoo, B. J.; Jonkheijm, P.; Brunsveld, L. Directed Supramolecular Surface Assembly of SNAP-tag Fusion Proteins. *Chem.—Eur. J.* **2012**, *18*, 6788−6794.

(11) Duan, X.; Rajan, N. K.; Routenberg, D. A.; Huskens, J.; Reed, M. A. Regenerative Electronic Biosensors Using Supramolecular Approaches. *ACS Nano* **2013**, *7*, 4014−4021.

(12) Soylemez, S.; Hacioglu, S. O.; Kesik, M.; Unay, H.; Cirpan, A.; Toppare, L. A Novel and Effective Surface Design: Conducting Polymer/β-Cyclodextrin Host−Guest System for Cholesterol Biosensor. *ACS Appl. Mater. Interfaces* **2014**, *6*, 18290−18300.

(13) Leprêtre, S.; Chai, F.; Hornez, J.; Vermet, G.; Neut, C.; Descamps, M.; Hildebrand, H. F.; Martel, B. Prolonged Local Antibiotics Delivery from Hydroxyapatite Functionalised with Cyclodextrin Polymers. *Biomaterials* **2009**, *30*, 6086−6093.

(14) Van de Manakker, F.; Vermonden, T.; Van Nostrum, C. F.; Hennink, W. E. Cyclodextrin-based Polymeric Materials: Synthesis, Properties, and Pharmaceutical/Biomedical Applications. *Biomacromolecules* **2009**, *10*, 3157−3175.

(15) Shi, J.; Votruba, A. R.; Farokhzad, O. C.; Langer, R. Nanotechnology in Drug Delivery and Tissue Engineering: from Discovery to Applications. *Nano Lett.* **2010**, *10*, 3223−3230.

(16) Sobocinski, J.; Laure, W.; Taha, M.; Courcot, E.; Chai, F.; Simon, N.; Addad, A.; Martel, B.; Haulon, S.; Woisel, P.; Blanchemain, N.; Lyskawa, J. Mussel Inspired Coating of a Biocompatible Cyclodextrin based Polymer onto CoCr Vascular Stents. *ACS Appl. Mater. Interfaces* **2014**, *6*, 3575−3586.

(17) Ludden, M. J.; Mulder, A.; Tampé, R.; Reinhoudt, D. N.; Huskens, J. Molecular Printboards as a General Platform for Protein Immobilization: A Supramolecular Solution to Nonspecific Adsorption. *Angew. Chem.* **2007**, *119*, 4182−4185.

(18) Ludden, M. J.; Li, X.; Greve, J.; van Amerongen, A.; Escalante, M.; Subramaniam, V.; Reinhoudt, D. N.; Huskens, J. Assembly of Bionanostructures onto β-Cyclodextrin Molecular Printboards for Antibody Recognition and Lymphocyte Cell Counting. *J. Am. Chem. Soc.* **2008**, *130*, 6964−6973.

(19) González-Campo, A.; Eker, B.; Gardeniers, H. J.; Huskens, J.; Jonkheijm, P. A Supramolecular Approach to Enzyme Immobilization in Micro-channels. *Small* **2012**, *8*, 3531−3537.

(20) Wasserberg, D.; Uhlenheuer, D. A.; Neirynck, P.; Cabanas-Danés, J.; Schenkel, J. H.; Ravoo, B. J.; An, Q.; Huskens, J.; Milroy, L.; Brunsveld, L.; Jonkheijm, P. Immobilization of Ferrocene-Modified SNAP-Fusion Proteins. *Int. J. Mol. Sci.* **2013**, *14*, 4066−4080.

(21) Petersson, L.; Städe, L. W.; Brofelth, M.; Gärtner, S.; Fors, E.; Sandgren, M.; Vallkil, J.; Olsson, N.; Larsen, K. L.; Borrebaeck, C. A.; Duroux, L.; Wingren, C. Molecular Design of Recombinant scFv Antibodies for Site-Specific Photocoupling to β-Cyclodextrin in Solution and onto Solid Support. *Biochim. Biophys. Acta, Proteins Proteomics* **2014**, *1884*, 2164−2173.

(22) Jonkheijm, P.; Weinrich, D.; Schröder, H.; Niemeyer, C. M.; Waldmann, H. Chemical Strategies for Generating Protein Biochips. *Angew. Chem., Int. Ed.* **2008**, *47*, 9618−9647.

(23) Onclin, S.; Ravoo, B. J.; Reinhoudt, D. N. Engineering Silicon Oxide Surfaces Using Self-Assembled Monolayers. *Angew. Chem., Int. Ed.* **2005**, *44*, 6282−6304.

(24) Busse, S.; DePaoli, M.; Wenz, G.; Mittler, S. An Integrated Optical Mach−Zehnder Interferometer Functionalized by β-Cyclodextrin to Monitor Binding Reactions. *Sens. Actuators, B* **2001**, *80*, 116−124.

(25) Onclin, S.; Mulder, A.; Huskens, J.; Ravoo, B. J.; Reinhoudt, D. N. Molecular Printboards: Monolayers of β-Cyclodextrins on Silicon Oxide Surfaces. *Langmuir* **2004**, *20*, 5460−5466.

(26) González-Campo, A.; Hsu, S.; Puig, L.; Huskens, J.; Reinhoudt, D. N.; Velders, A. H. Orthogonal Covalent and Noncovalent Functionalization of Cyclodextrin-Alkyne Patterned Surfaces. *J. Am. Chem. Soc.* **2010**, *132*, 11434−11436.

(27) Piehler, J.; Brecht, A.; Hehl, K.; Gauglitz, G. Protein Interactions in Covalently Attached Dextran Layers. *Colloids Surf., B* **1999**, *13*, 325−336.

(28) De Sousa Delgado, A.; Leonard, M.; Dellacherie, E. Surface Properties of Polystyrene Nanoparticles Coated with Dextrans and Dextran-PEO Copolymers. Effect of Polymer Architecture on Protein Adsorption. *Langmuir* **2001**, *17*, 4386−4391.

(29) Martwiset, S.; Koh, A. E.; Chen, W. Nonfouling Characteristics of Dextran-Containing Surfaces. *Langmuir* **2006**, *22*, 8192−8196.

(30) Nielsen, T. T.; Wintgens, V.; Amiel, C.; Wimmer, R.; Larsen, K. L. Facile Synthesis of β-Cyclodextrin-Dextran Polymers by "Click" Chemistry. *Biomacromolecules* **2010**, *11*, 1710−1715.

(31) Chan, T. R.; Hilgraf, R.; Sharpless, K. B.; Fokin, V. V. Polytriazoles as Copper (I)-Stabilizing Ligands in Catalysis. *Org. Lett.* **2004**, *6*, 2853−2855.

(32) Das, B.; Reddy, V. S.; Tehseen, F.; Krishnaiah, M. Catalyst-Free Highly Regio-and Stereoselective Ring Opening of Epoxides and Aziridines with Sodium Azide Using Poly(ethylene glycol) as an Efficient Reaction Medium. *Synthesis* **2007**, *5*, 666−668.

(33) Luzinov, I.; Julthongpiput, D.; Liebmann-Vinson, A.; Cregger, T.; Foster, M. D.; Tsukruk, V. V. Epoxy-Terminated Self-Assembled Monolayers: Molecular Glues for Polymer Layers. *Langmuir* **2000**, *16*, 504−516.

(34) Meldal, M.; Tornøe, C. W. Cu-Catalyzed Azide-Alkyne Cycloaddition. *Chem. Rev.* **2008**, *108*, 2952−3015.

(35) Rekharsky, M. V.; Inoue, Y. Complexation Thermodynamics of Cyclodextrins. *Chem. Rev.* **1998**, *98*, 1875−1918.

(36) Kawaguchi, T.; Hasegawa, M. Structure of Dextran−Magnetite Complex: Relation between Conformation of Dextran Chains Covering Core and its Molecular Weight. *J. Mater. Sci. Mater. Med.* **2000**, *11*, 31−35.

(37) Frazier, R.; Matthijs, G.; Davies, M.; Roberts, C.; Schacht, E.; Tendler, S. Characterization of Protein-resistant Dextran Monolayers. *Biomaterials* **2000**, *21*, 957−966.

(38) Lummerstorfer, T.; Hoffmann, H. Click Chemistry on Surfaces: 1, 3-Dipolar Cycloaddition Reactions of Azide-Terminated Monolayers on Silica. *J. Phys. Chem. B* **2004**, *108*, 3963−3966.

DOI: 10.1021/am508350r
ACS Appl. Mater. Interfaces 2015, 7, 4160−4168

(39) Catena, G. C.; Bright, F. V. Thermodynamic Study on the Effects of β-Cyclodextrin Inclusion with Anilinonaphthalenesulfonates. *Anal. Chem.* **1989**, *61*, 905−909.
(40) Fülöp, Z.; Nielsen, T. T.; Larsen, K. L.; Loftsson, T. Dextran-Based Cyclodextrin Polymers: Their Solubilizing Effect and Self-Association. *Carbohydr. Polym.* **2013**, *97*, 635−642.
(41) Gonzalez-Gaitano, G.; Rodriguez, P.; Isasi, J.; Fuentes, M.; Tardajos, G.; Sánchez, M. The Aggregation of Cyclodextrins as Studied by Photon Correlation Spectroscopy. *J. Inclusion Phenom. Macrocyclic Chem.* **2002**, *44*, 101−105.
(42) Messner, M.; Kurkov, S. V.; Jansook, P.; Loftsson, T. Self-Assembled Cyclodextrin Aggregates and Nanoparticles. *Int. J. Pharm.* **2010**, *387*, 199−208.
(43) Marcus, Y. Effect of Ions on the Structure of Water: Structure Making and Breaking. *Chem. Rev.* **2009**, *109*, 1346−1370.
(44) Curry, S.; Mandelkow, H.; Brick, P.; Franks, N. Crystal Structure of Human Serum Albumin Complexed with Fatty Acid Reveals an Asymmetric Distribution of Binding Sites. *Nat. Struct. Mol. Biol.* **1998**, *5*, 827−835.

DOI: 10.1021/am508350r
ACS Appl. Mater. Interfaces 2015, 7, 4160−4168